Industrial Engineering & Management

Trivedi et al., Ind Eng Manage 2015, 4:5
DOI: 10.4172/2169-0316.1000177

Research Article Open Access

Evaluation of Thermal and Physical Properties of Magnesium Nitride Powder: Impact of Biofield Energy Treatment

Mahendra Kumar Trivedi[1], Rama Mohan Tallapragada[1], Alice Branton[1], Dahryn Trivedi[1], Gopal Nayak[1], Omprakash Latiyal[2] and Snehasis Jana[2]*

[1]*Trivedi Global Inc., 10624 S Eastern Avenue Suite A-969, Henderson, NV 89052, USA*

[2]*Trivedi Science Research Laboratory Pvt. Ltd., Hall-A, Chinar Mega Mall, Chinar Fortune City, Hoshangabad Rd., Bhopal-462026, Madhya Pradesh, India*

Abstract

Magnesium nitride (Mg_3N_2) has gained extensive attention due to its catalytic and optoelectronic properties. The present investigation was aimed to evaluate the effect of biofield energy treatment on physical and thermal properties of Mg_3N_2 powder. The Mg_3N_2 powder was divided into two parts i.e. control and treated. The control part was remained as untreated and the treated part was subjected to the Mr. Trivedi's biofield energy treatment. Subsequently, the control and treated Mg_3N_2 samples were characterized using differential scanning calorimetry (DSC), thermogravimetric analysis (TGA), and X-ray diffraction (XRD). The DSC results showed the specific heat capacity of 2.24 $Jg^{-1}°C^{-1}$ in control, which increased upto 5.55 $Jg^{-1}°C^{-1}$ in treated Mg_3N_2 sample. The TGA data revealed that the onset temperature for the formation of magnesium oxide, possibly due to oxidation of Mg_3N_2 in the presence of air and moisture, was reduced from 421.0°C (control) to 391.33°C in treated sample. Besides, the XRD data revealed that the lattice parameter and unit cell volume of treated Mg_3N_2 samples were increased by 0.20 and 0.61% respectively, as compared to the control. The shifting of all peaks toward lower Bragg angle was observed in treated sample as compared to the control. The XRD diffractogram also showed that the relative intensities of all peaks were altered in treated sample as compared to control. In addition, the density of treated Mg_3N_2 was reduced by 0.60% as compared to control. Furthermore, the crystallite size was significantly increased from 108.05 nm (control) to 144.04 nm in treated sample as compared to the control. Altogether data suggest that biofield energy treatment has substantially altered the physical and thermal properties of Mg_3N_2 powder. Thus, the biofield treatment could be applied to modulate the catalytic and optoelectronic properties of Mg_3N_2 for chemical and semiconductor industries.

Keywords: Biofield energy treatment; Magnesium nitride powder; X-ray Diffraction; DSC; TGA

Introduction

Magnesium nitride (Mg_3N_2) is well-known for its role as an additive in a range of applications, including fabricating special alloys and ceramics, catalyzing polymer cross-linking reactions etc. [1]. Generally, Mg_3N_2 is applied as catalysts to prepare some metal nitrides or non-metal nitrides, especially cubic boron nitride. It is a convenient source of ammonia in the preparation of primary amides and dihydropyridines [2]. Recently, Mg_3N_2 powder has shown enormous potential for fabricating hydrogen storage materials [3]. In addition, it is also used in the formation of high thermal conductivity ceramics [4]. It has attracted considerable interest in optoelectrical field due to its direct band gap of 1.1 to 2.5 eV [5]. Besides, in catalytic activities of Mg_3N_2, its thermal and physical characteristics play a vital role. Recently, researcher have used various processes to prepare Mg_3N_2 powder with desired physical and thermal properties such as Mg direct reaction with NH_3 [1], low pressure chemical vapor deposition method [6], and electrochemical process [7] etc. All these process required either expensive equipment or high power and energy sources to control its thermal and physical properties. Thus, after conceiving the vast importance of Mg_3N_2 in several industries, authors wish to investigate an approach that could be beneficial to modify the physical and thermal properties of Mg_3N_2 powder.

It is well established that the energy can effectively interact with any matter at a distance and cause action. The energy is exist in various fields such as electric, magnetic etc. Furthermore, researchers have confirmed that biomagnetic fields are present around the human body, which has been evidenced by electromyography (EMG), electrocardiography (ECG) and electroencephalogram (EEG) [8,9]. Moreover, a human has the ability to harness the energy from environment/universe and can transmit it to any object (living or non-living) around the Globe. The object(s) always receive the energy and responded into useful way that is called biofield energy. This process is termed as biofield energy treatment. The National Center for Complementary and Alternative Medicine (NCCAM) considered the biofield treatment (or healing therapy) under subcategory of energy therapies [10,11]. Mr. Trivedi's unique biofield energy treatment is known as The Trivedi Effect®. Mr. Trivedi's biofield energy treatment is known to alter the physical, structural and atomic characteristic in several metals [12-14] and ceramics [15,16]. Our group previously reported that biofield treatment has substantially altered the lattice parameter, crystallite size, and particle size in silicon carbide [17] and manganese oxide [18]. Hence, based on the outstanding results accomplished by biofield energy treatment on metals and ceramics, an attempt was made to evaluate the effect of biofield treatment on thermal and physical properties of Mg_3N_2 powder using differential scanning calorimetry (DSC), thermogravimetric analysis (TGA), and X-ray diffraction (XRD).

***Corresponding author:** Snehasis Jana, Trivedi Science Research Laboratory Pvt. Ltd., Hall-A, Chinar Mega Mall, Chinar Fortune City, Hoshangabad Rd., Bhopal-462026, Madhya Pradesh, India, Tel: +91-755-6660006; E-mail: publication@trivedieffect.com

Received September 14, 2015; **Accepted** October 21, 2015; **Published** October 23, 2015

Citation: Trivedi MK, Tallapragada RM, Branton A, Trivedi D, Nayak G, et al. (2015) Evaluation of Thermal and Physical Properties of Magnesium Nitride Powder: Impact of Biofield Energy Treatment. Ind Eng Manage 4: 177. doi:10.4172/2169-0316.1000177

Methods

The Mg_3N_2 powder was purchased from Sigma Aldrich, India. The powder was equally divided into two parts, referred as control and treated. The treated group was in sealed pack and handed over to Mr. Trivedi for biofield energy treatment under standard laboratory condition. Mr. Trivedi provided the biofield treatment through his energy transmission process to the treated group without touching the sample. The control and treated samples were characterized using DSC, TGA and XRD.

DSC analysis

The thermal analysis of Mg_3N_2 powder was performed using DSC. For DSC study, Pyris-6 Perkin Elmer, with a heating rate of 10°C/min under nitrogen atmosphere was used. The specific heat capacity of Mg_3N_2 powder was calculated from the DSC curve.

TGA-DTG analysis

TGA analysis was carried out using Mettler Toledo TGA-DTG system. The samples were heated from room temperature to 900°C with a heating rate of 10°C/min. The change in weight of the sample was observed in TGA curve, whereas the DTG curve provided the T_{max}, where sample lost maximum of its weight.

XRD study

The XRD analysis of control and treated Mg_3N_2 powder was carried out on Phillips, Holland PW 1710 X-ray diffractometer system. It had a copper anode with nickel filter. The radiation of wavelength used by the XRD system was 1.54056Å. This XRD system provided the data in the form of a chart of 2θ *vs.* intensity and a detailed table containing peak intensity counts, d value (Å), peak width (θ°), relative intensity (%) etc. Further, the PowderX software was used to calculate lattice parameter and unit cell volume of Mg_3N_2 powder samples. The weight of the unit cell was calculated as, molecular weight multiplied by the number of atoms present in a unit cell. Also, the density of the unit cell was computed as follows:

$$\text{Density} = \frac{\text{Weight of unit cell}}{\text{Volume of unit cell}}$$

The crystallite size (G) was calculated by using Scherrer equation as given below:

$$\text{Crystallite size (G)} = k\lambda/(b\,\text{Cos}\theta),$$

Here, λ is the wavelength of radiation used, k is the equipment constant (0.94) and b is full width half maximum (FWHM) and, θ is Bragg's angle.

Besides, the percent change in the unit cell volume was calculated using following equation:

$$\%\,\text{change in unit cell volume} = \frac{[V_{\text{Treated}} - V_{\text{Control}}]}{V_{\text{Control}}} \times 100$$

Where $V_{Control}$ and $V_{Treated}$ are the unit cell volume of control and treated samples respectively. Similarly, the percent change in all other parameters such as lattice parameter, density, molecular weight, and crystallite size were calculated.

Results and Discussion

DSC analysis

The DSC was employed to study the thermal characteristics of control and treated Mg_3N_2 powders. For DSC analysis, treated part was divided into three parts, considered as T1, T2, and T3. Figures 1a-1d shows the DSC curves of control and treated Mg_3N_2 samples. From the DSC curve, the heat absorbed (ΔH) during rise in temperature was recorded, which was further used to compute the specific heat capacity of samples. The DSC curve showed a broad peak in control sample, which was started from 285.09°C and ended at 363.45°C. However, treated T1 sample also exhibited the broad peak, which started from 269.74°C and ended at 354.24°C. Similarly, T2 and T3 showed the onset at 297.88°C and 297.57°C and endset at 407.80°C and 382.42°C, respectively. In addition, the peak temperature in this process was found to be 342.47°C, 329.84°C, 355.63°C, and 349.9°C in control, T1, T2, and T3 respectively. Furthermore, the heat absorbed (ΔH) by the control samples during temperature rise (285→363.45°C) was 175.6 J/g. However, the heat absorbed by treated samples T1, T2, and T3 were 277.6 J/g (299.74→354.84°C), 610.1 J/g (297.88→407.80°C), and 479.7 J/g (297.57→382.42°C), respectively (Table 1). It indicated that the ΔH was increased by 58.03, 247.36, and 173.3 % in treated T1, T2, and T3, respectively as compared to the control (Figure 2). In addition, the specific heat capacity (C_p) i.e. the heat required to raise the temperature

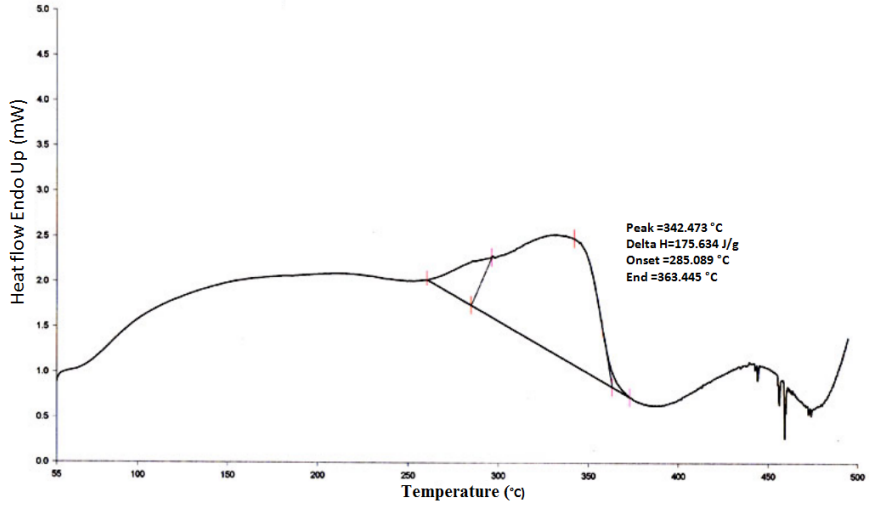

Figure 1a: DSC curve of control magnesium nitride sample.

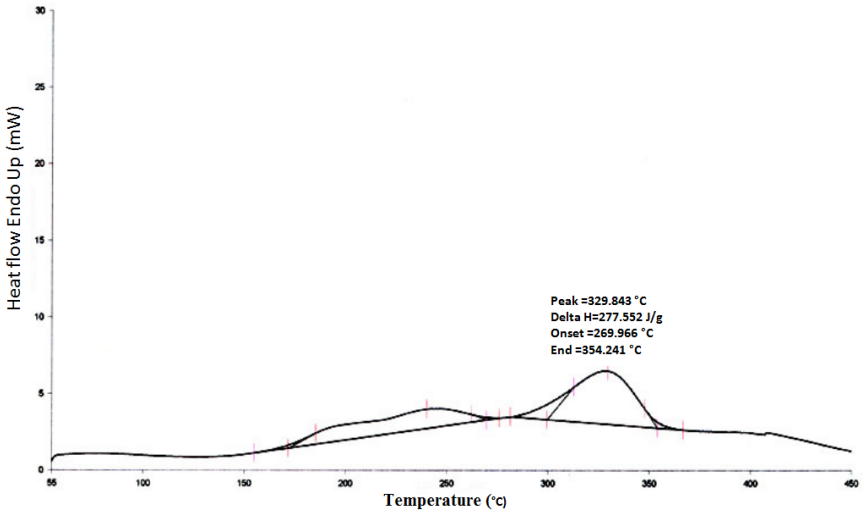

Figure 1b: DSC curve of treated (T1) magnesium nitride sample.

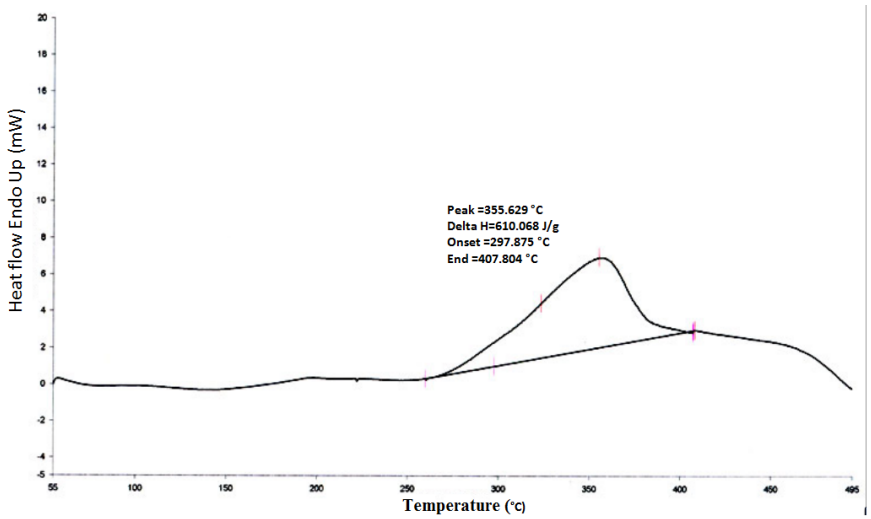

Figure 1c: DSC curve of treated (T2) magnesium nitride sample.

	Onset Temperature (°C)	Peak Temperature (°C)	Endset Temperature (°C)	ΔH (J/g)	Specific heat capacity, C_p ($Jg^{-1}°C^{-1}$)
Control	285.09	342.47	363.45	175.6	2.24
T1	269.74	329.84	354.24	277.6	5.09
T2	297.88	355.63	407.80	610.1	5.55
T3	297.57	349.9	382.42	479.7	5.65

T: Trearted; ΔH: Heat absorbed by sample

Table 1: DSC analysis of magnesium nitride powder.

of one gram substance by one degree Celsius, was 2.24 $Jg^{-1}°C^{-1}$ in the control Mg_3N_2 sample, which was significantly increased to 5.09, 5.55, and 5.65 J $g^{-1}°C^{-1}$ in T1, T2, and T3 samples, respectively. It indicated that C_p was substantially increased by 127.22, 147.63, and 152.23% in treated T1, T2, and T3 samples, respectively as compared to the control. Moreover, our group previously reported that biofield treatment had altered the latent heat of fusion in cadmium powder [19]. The specific heat capacity is depended on the number of degrees of freedom. Like the molecule with n atom have 3n number of degrees of freedom [20]. Thus, Mg_3N_2 has 15 number of degrees of freedom. Each degree of freedom allows the particle to store thermal energy. In addition, the translation kinetic energy of the particle is one of the possible degrees of freedom, which manifests to the change in temperature [21]. Thus, based on this, it is assumed that biofield treatment possibly altered the energy associated with degrees of freedom other than kinetic energy such as rotational, vibrational etc. This might be the probable reason

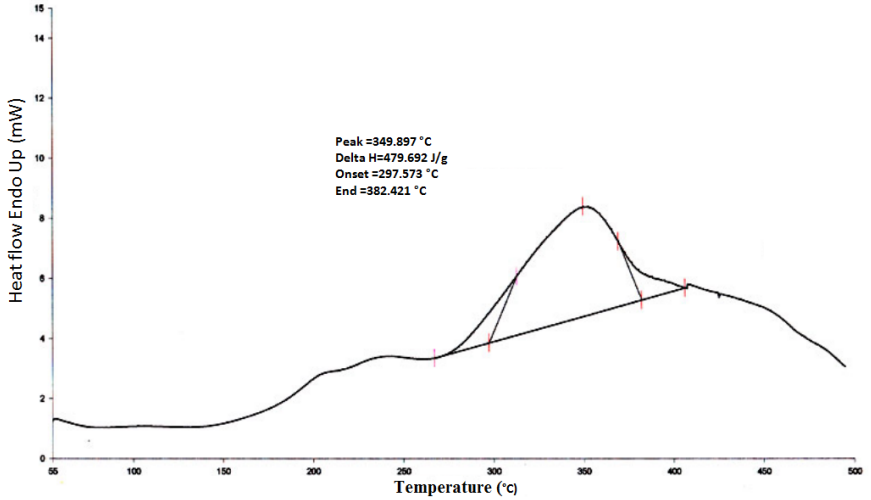

Figure 1d: DSC curve of treated (T3) magnesium nitride sample.

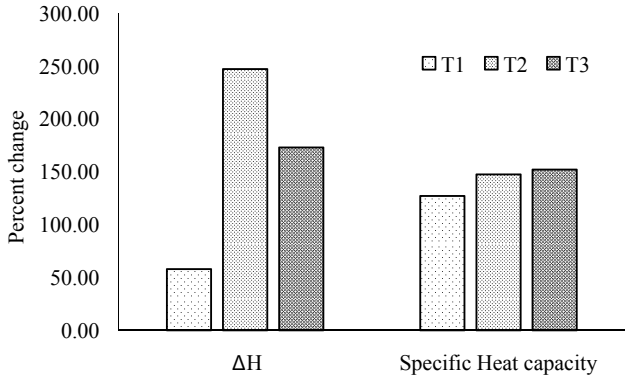

Figure 2: Effect of biofield treatment on thermal properties of magnesium nitride.

for change in specific heat capacity of treated Mg_3N_2 powder.

TGA analysis

The TGA analysis of Mg_3N_2 powder was carried out in the temperature range 0-900°C, under nitrogen atmosphere. Figure 3 shows the TGA curve of control and treated Mg_3N_2 samples. The control sample showed that the sample lost 4.10% of its initial weight till 421°C, afterward the weight of the sample was continuously increased. It was reported that the reduction in weight loss of Mg_3N_2 in TGA curve in N_2 atmosphere under 500°C was due to the release of H_2O, CO_2, N_2 and O_2 from the surface of powder [22]. However, the weight of the sample was started to increase after 421°C. It is reported that during TGA analysis, the presence of water and oxygen oxidises the Mg_3N_2 to MgO and increase the weight of the sample [23]. The DTG showed the control sample gained its maximum weight at 582.33°C, possibly due to oxidation of Mg_3N_2. Furthermore, the control sample was continued to gain the weight by 4.25% till temperature reach to 657.47°C. However, the treated sample lost its weight of 2.66% upto 391.33°C, possibly due to release of H_2O, CO_2, N_2 and O_2 from the surface of powder. After that the treated sample was started to gain the weight at 391.33°C that might be due to oxidation of Mg_3N_2. The DTG showed that sample

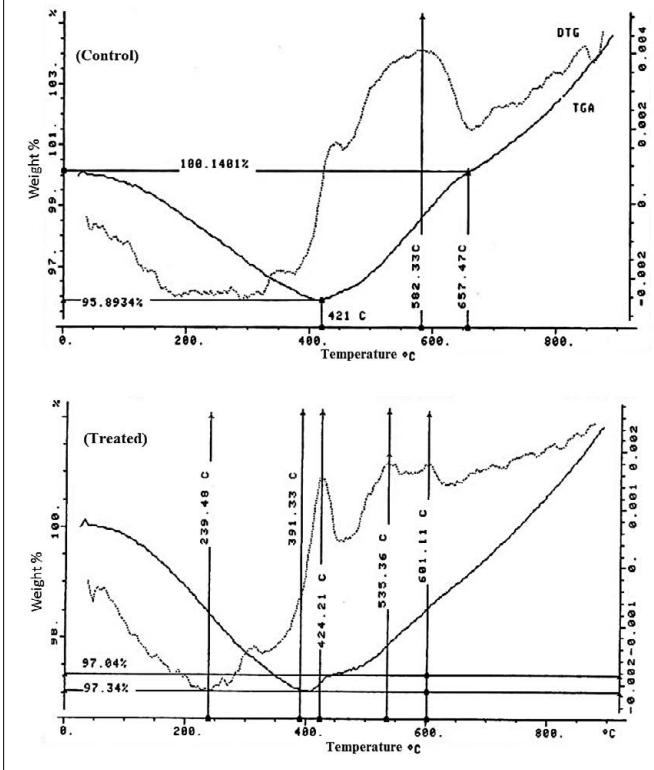

Figure 3: TGA curve of magnesium nitride powder.

showed the three different peaks corresponding to weight gain at i.e. at 424.21°C, 535°C, and 601.11°C. Moreover, in order to find out the probable cause for the alteration in thermal properties, the control and treated Mg_3N_2 samples were examined using XRD.

X-ray diffraction (XRD)

XRD is a non-destructive and quantitative technique, which has been extensively used to determine the crystal structure parameters

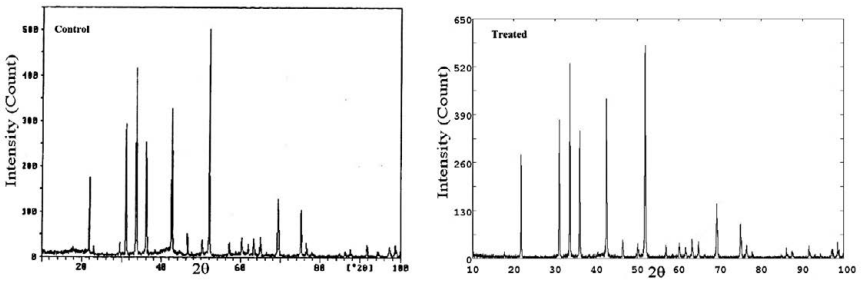

Figure 4: XRD diffractogram of magnesium nitride powder.

Plane (hkl)	Control		Treated	
	2 θ (Degree)	Relative Intensity	2 θ (Degree)	Relative Intensity
211	21.89	31.7	21.80	44.6
222	31.10	50.4	31.03	67.8
321	33.67	76.5	33.58	97.4
400	36.05	43.9	35.97	65.7
332	42.57	58.7	42.47	79.6
531	51.91	100	51.81	100
440	52.08	41.6	51.98	51.8
721	69.31	27	69.21	22.5
732	75.05	18.4	74.97	16.8

Table 2: Effect of biofield energy treatment on the Bragg angle (2θ) and relative intensities of XRD peaks of magnesium nitride powder.

Group	Lattice parameter (Å)	Unit cell volume ($\times 10^{-23} cm^3$)	Density (g/cc)	Molecular weight (g/mol)	Crystallite size (nm)
Control	9.9551	98.6586	2.716	100.855	108.05
Treated	9.9752	99.2586	2.699	101.469	144.04
Percent change	0.20	0.61	-0.60	0.61	33.30

Table 3: Effect of biofield energy treatment on the lattice parameter, unti cell volume, density, molecular weight and crystallite size of magnesium nitride.

such as lattice parameters, unit cell volume etc. The XRD diffractogram of control and treated Mg_3N_2 samples are presented in Figure 4. The control sample showed the crystalline peaks at 2θ equal to 21.89°, 31.10°, 33.67°, 36.05°, 42.57°, 51.91°, 52.08°, 69.31°, and 75.05°, which were indexed to the crystalline plane (211), (222), (321), (400), (332), (531), (440), (721), and (732) respectively, according to Joint Committee on Powder Diffraction Standards (JCPDS) card No. 35-0778 [24]. However, treated sample showed crystalline peaks at 21.80°, 31.03°, 33.58°, 35.97°, 42.47°, 51.81°, 51.98°, 69.21°, and 74.97°. This indicated that all peaks in the treated sample were shifted to lower Bragg angle as compared to the control. Also, the peak corresponding to plane (531) was found to be the most intense among other peaks in both control and treated samples. Further, the relative intensities of all peaks in control and treated sample were summarized in Table 2. The data showed that relative intensities of all peaks were significantly altered in the treated sample as compared to the control. Inoue et al. reported that the change in crystal morphology leads to alter the relative intensities of XRD peaks [25]. Also, our group reported that the biofield treatment had altered the particle size, and surface morphology in zinc [10] and antimony powder [11]. Thus, it is possible that the size, shape and surface morphology of treated Mg_3N_2 might alter after biofield treatment and that might be the probable cause for the alteration in relative intensities in treated sample. Furthermore, the crystal structure parameters such as lattice parameter, unit cell volume, density and molecular weight were computed and presented in Table 3. The data exhibited that the lattice parameter of unit cell was increased by 0.20% in treated sample as compared to the control. Hirai et al. reported that the stress (or pressure) on the compounds causes the alteration in relative intensities and lattice strain [26]. It is also reported that increase in lattice parameter leads to shift the XRD peaks toward lower Bragg angle and vice versa [27]. Hence, the increase in lattice parameter was supported by the shifting of XRD peaks toward lower Bragg's angle in treated Mg_3N_2 sample. Paszkowicz et al. reported that the lattice parameter of Mg_3N_2 was increased by 0.14%, when temperature was raised from 1 K up to 304.5 K. It is mentioned that the change in lattice parameter caused the alteration in the thermal expansion coefficient of the compound [28]. Thus, it is assumed that the change in lattice parameter i.e. distance between two atoms might be responsible for the alteration in thermal properties. Besides, the increase in lattice parameter led to increase the unit cell volume by 0.61% in treated sample as compared to the control. In relation to this, the change in lattice parameter is also known as lattice strain (ε), which is related to stress (σ) by following equation [29]:

$$\sigma = Y\varepsilon$$

Where Y is Young's Modulus

In above equation, the negative strain indicated the compressive stress, whereas positive strain is related to tensile stress. Thus, the positive lattice strain found in treated Mg_3N_2 sample suggests that biofield treatment might induce tensile stress and that might be the responsible for alteration in lattice parameter and unit cell volume. Besides, the increase in unit cell volume led to reduce the density by 0.60% in the treated Mg_3N_2 sample as compared to the control. Contrarily, the molecular weight of treated Mg_3N_2 was increased from 100.855 g/mol (control) to 101.469 g/mol. It is already reported that biofield treatment has significantly altered the atomic weight and density in silicon carbide [17]. Furthermore, the crystallite size of control and treated Mg_3N_2 powder were computed using Scherrer equation and calculated result are presented in Table 3. The crystallite size was increased from 108.05 nm (control) to 144.04 nm in treated sample. It suggests that the crystallite size of treated Mg_3N_2 powder was significantly increased by 33.30% as compared to the control. The increase in crystallite size could be due to the movement of crystallite boundaries in treated sample after biofield treatment. It is possible that the energy, which probably transferred through biofield treatment might induce the movements of dislocation present at crystallite boundaries.

Conclusions

In summary, the biofield energy treatment has substantially altered the specific heat capacity, crystallite size, and unit cell parameters. The specific heat capacity of treated Mg_3N_2 was significantly increased up to 152.23% as compared to the control. The biofield treatment showed the alteration in the lattice parameter (0.20%), unit cell volume (0.61%), density (-0.60%), and molecular weight (0.61%) in treated sample as compared to control. On the basis of alteration in relative intensities of XRD peaks in treated sample as compared to control, it is concluded that the biofield energy treatment probably altered the surface morphology of the treated Mg_3N_2 powder. In addition, the crystallite size of the treated sample was significantly increased by 33.30% as compared to control. Therefore, based on the above outcomes it is concluded that biofield treated Mg_3N_2 could be more useful in chemical and optoelectronic properties.

Acknowledgement

Authors gratefully acknowledged Dr. Cheng Dong of NLSC from Institute of Physics, and Chinese academy of sciences for providing the facilities to use PowderX software for analyzing XRD data. Authors also would like to thank Trivedi science, Trivedi master wellness and Trivedi testimonials for their support during the work.

References

1. Xue CS, Ai YJ, Sun LL (2007) Synthesis and photoluminescence properties of Mg_3N_2 powders. Rare Met Mater Eng 36: 2020-2022.
2. Veitch GE, Bridgwood KL, Rands-Trevor K, Ley SV (2008) Magnesium nitride as a convenient source of ammonia: preparation of pyrroles. Synlett 2008: 2597-2600.
3. Kojima Y, Kawai Y, Ohba N (2006) Hydrogen storage of metal nitrides by a mechanochemical reaction. J Power Sources 159: 81-87.
4. Nakano S, Ikawa H, Fukunaga O (1993) High pressure reactions and formation mechanism of cubic BN in the system BN Mg_3N_2. Diamond Relat Mater 2: 1168-1174.
5. Armenta MGM, Reyes-Serrato A, Borja MA (2000) Ab initio determination of the electronic structure of beryllium-, aluminum-, and magnesium-nitrides: A comparative study. Phys Rev B 62: 4890.
6. Murata T, Itatani K, Howell FS, Kishioka A, Kinoshita M (1993) Preparation of magnesium nitride powder by low-pressure chemical vapor deposition. J Am Ceram Soc 76: 2909-2911.
7. Toyoura K, Goto T, Hachiya K, Hagiwara R (2005) Structural and optical properties of magnesium nitride formed by a novel electrochemical process. Electrochim Acta 51: 56-60.
8. Movaffaghi Z, Farsi M (2009) Biofield therapies: Biophysical basis and biological regulations. Complement Ther Clin Pract 15: 35-37.
9. Priyadarsini K, Thangam P, Gunasekaran S (2014) Kirlian images in medical diagnosis: A survey. IJCA Proceedings on International Conference on Simulations in Computing Nexus 3: 5-7.
10. Aldridge D (1991) Spirituality, healing and medicine. Br J Gen Pract 41: 425-427.
11. Hok J, Tishelman C, Ploner A, Forss A, Falkenberg T (2008) Mapping patterns of complementary and alternative medicine use in cancer: an explorative cross-sectional study of individuals with reported positive “exceptional” experiences. BMC Complement Altern Med 8: 48.
12. Trivedi MK, Tallapragada RM (2008) A transcendental to changing metal powder characteristics. Met Powder Rep 63: 22-28, 31.
13. Dhabade VV, Tallapragada RM, Trivedi MK (2009) Effect of external energy on atomic, crystalline and powder characteristics of antimony and bismuth powders. Bull Mater Sci 32: 471-479.
14. Trivedi MK, Tallapragada RM, Branton A, Trivedi D, Nayak G, et al. (2015) Potential impact of biofield treatment on atomic and physical characteristics of magnesium. Vitam Miner 3: 129.
15. Trivedi MK, Nayak G, Patil S, Tallapragada RM, Latiyal O (2015) Studies of the atomic and crystalline characteristics of ceramic oxide nano powders after bio field treatment. Ind Eng Manage 4: 161.
16. Trivedi MK, Nayak G, Patil S, Tallapragada RM, Latiyal O, et al. (2015) Impact of biofield treatment on atomic and structural characteristics of barium titanate powder. Ind Eng Manage 4: 166.
17. Trivedi MK, Nayak G, Tallapragada RM, Patil S, Latiyal O, et al. (2015) Effect of biofield treatment on structural and morphological properties of silicon carbide. J Powder Metall Min 4: 132.
18. Trivedi MK, Nayak G, Patil S, Tallapragada RM, Latiyal O (2015) Evaluation of biofield treatment on physical, atomic and structural characteristics of manganese (II, III) oxide. J Material Sci Eng 4: 177.
19. Trivedi MK, Nayak G, Patil S, Tallapragada RM, Latiyal O, et al. (2015) An evaluation of biofield treatment on thermal, physical and structural properties of cadmium powder. J Thermodyn Catal 6: 147.
20. Curry JA, Webster PJ (1999) Thermodynamics of atmospheres and ocean. Academic Press Medical.
21. Wiberg E, Wiberg N (2001) Inorganic chemistry. Academic Press. Science.
22. Zong F, Meng C, Guo Z, Ji F, Xiao H (2010) Synthesis and characterization of magnesium nitride powder formed by Mg direct reaction with N_2. J Alloy Compd 508 172-176.
23. Kim D, Kim T, Park H, Park D (2011) Synthesis of nanocrystalline magnesium nitride (Mg_3N_2) powder using thermal plasma Appl Surf Sci 257: 5375-5379.
24. Mei L, Li JT (2009) Combustion synthesis of ultrafine magnesium nitride powder by Ar dilution. Scripta Mater 60: 141-143.
25. Inoue M, Hirasawa I (2013) The relationship between crystal morphology and XRD peak intensity on $CaSO_4 \cdot 2H_2O$. J Cryst Growth 380: 169-175.
26. Hirai H, Kondo T, Hasegawa M, Yagi T, Sakashita M, et al. (2000) Structural changes of methane hydrate under high pressure at room temperature. High pressure (Science).
27. Mohapatra J (2013) Defect-related blue emission from ultra-fine Zn1−xCdxS quantum dots synthesized by simple beaker chemistry. Int Nano Lett 3:31.
28. Paszkowicz W, Knapp M, Domagala JZ, Kamler G, Podsiadlo S (2001) Low-temperature thermal expansion of Mg_3N_2. J Alloy Compd 328: 272-275.
29. Soboyejo W (2002) Mechanical properties of engineered materials. CRC press.